Translationally invariant density

Petr Navrátil
Lawrence Livermore National Laboratory, L-414, P.O. Box 808, Livermore, California 94551, USA
(Received 23 May 2004; published 30 July 2004)

Translationally invariant nuclear density is derived from the shell model one-body densities by removing their spurious $0\hbar\Omega$ center-of-mass (c.m.) motion component. This paves the way to utilizing the *ab initio* no-core shell-model (NCSM) nuclear structure in folding approaches to optical potentials. As an illustration, the ^{6}He diagonal and transitional densities are calculated from the NCSM wave functions obtained using the CD-Bonn nucleon-nucleon potential in the $10\hbar\Omega$ basis space. A particularly significant impact of the exact removal of the spurious c.m. motion is found for the spin-orbit part of the optical potential proportional to the derivative of the nuclear density.

DOI: 10.1103/PhysRevC.70.014317 PACS number(s): 21.60.Cs, 24.50.+g, 21.30.Fe

I. INTRODUCTION

There has been significant progress in the *ab initio* approaches to the structure of light nuclei. Starting from the realistic two- and three-nucleon interactions, methods like the Green's function Monte Carlo (GFMC) [1] or the *ab initio* no-core shell model (NCSM) [2] can predict the low-lying levels in *p*-shell nuclei.

The principal foundation of the *ab initio* NCSM approach is the use of effective interactions appropriate for the large but finite basis spaces employed in the calculations. These effective interactions are derived from the underlying realistic internucleon potentials through a unitary transformation in a way that guarantees convergence to the exact solution as the basis size increases. For the basis, one uses antisymmetrized *A*-nucleon harmonic-oscillator (HO) states that span the complete $N_{\max}\,\hbar\Omega$ space. A disadvantage of the HO basis is its unphysical asymptotic behavior. On the other hand, the nuclear system is translationally invariant and, particularly in the case of light nuclei, it is important to preserve this symmetry. The HO basis is the only basis that allows a switch from Jacobi coordinates to single-particle Cartesian coordinates without violating the translational invariance. Consequently, one may choose the coordinates according to whatever is more efficient for the problem at hand. In practice, it turns out that the $A=3$ system is the easiest solved in the Jacobi basis, the $A=4$ system can be solved either way with the same efficiency when only the two-body interaction is utilized, but the Jacobi basis is more efficient when the three-body interaction is included. For systems with $A>4$, it is by far more advantageous to use the Cartesian coordinates and the Slater determinant (SD) basis, and employ the powerful shell model codes like Antoine [3] that rely on the second quantization techniques.

While the NCSM eigenenergies are independent on the choice of coordinates, the eigenfunctions obtained in the Cartesian-coordinate SD basis include a $0\hbar\Omega$ spurious center-of-mass (c.m.) component. The ways to remove these components and obtain physical matrix elements of different operators were investigated in the past [4–10]. Typically, in earlier investigations the basis space was limited to a single major HO shell. In the NCSM, the basis space spans several major shells. Unlike in some phenomenological shell-model studies that used a multimajor shell basis, the c.m. motion is completely separated from the internal motion due to the translational invariance of the interactions and the choice of the complete $N_{\max}\,\hbar\Omega$ HO basis, as already discussed. In general, it is necessary to revisit and adapt the techniques of the spurious c.m.. motion removal to make them applicable for the NCSM. This paper, in particular, focuses on the construction of the translationally invariant density starting from the Cartesian-coordinate SD wave functions. This case is much less trivial than, e.g., the removal of spurious components from spectroscopic amplitudes.

The motivation for this work is the desire to apply the *ab initio* NCSM nuclear structure to describe nuclear reactions on light nuclei. In general, it is a challenging task to extend the *ab initio* methods to describe nuclear reactions. Concerning direct reactions, particularly the nucleon-nucleus elastic and inelastic scattering, a first and straightforward answer for the NCSM is the application of semimicroscopic approaches, e.g., the Jeukenne-Lejeune-Mahaux (JLM) [11], to construct optical potentials from the nuclear densities obtained in the NCSM. Eventually, these optical potentials are used in coupled-channel calculations by employing the standard codes, e.g., Fresco [12]. To fully utilize the NCSM nuclear structure for this purpose, the spurious c.m. contribution must be removed from the density. In Sec. II, the translational invariant density is derived from both the Jacobi-coordinate HO wave functions, as well as from the Cartesian-coordinate wave functions. In Sec. III, numerical tests for $A=3,4$, and 5 systems are described and an application to ^{6}He is presented. A spin-orbit part of the $p+^6$He optical potential is constructed to demonstrate the importance of the spurious c.m. removal. Conclusions are given in Sec. IV.

II. DERIVATION OF THE TRANSLATIONALLY INVARIANT DENSITY

A. Coordinate and HO wave-function transformations

We follow the notation of Ref. [13]. We consider nucleons with the mass *m* neglecting the difference between the proton and the neutron mass. For the purpose of the present paper we use the following set of Jacobi coordinates:

$$\vec{\xi}_0 = \sqrt{\frac{1}{A}}[\vec{r}_1 + \vec{r}_2 + \ldots + \vec{r}_A], \tag{1a}$$

$$\vec{\xi}_1 = \sqrt{\frac{1}{2}}[\vec{r}_1 - \vec{r}_2], \tag{1b}$$

$$\vec{\xi}_2 = \sqrt{\frac{2}{3}}\left[\frac{1}{2}(\vec{r}_1 + \vec{r}_2) - \vec{r}_3\right], \tag{1c}$$

$$\ldots$$

$$\vec{\xi}_{A-2} = \sqrt{\frac{A-2}{A-1}}\left[\frac{1}{A-2}(\vec{r}_1 + \vec{r}_2 + \ldots + \vec{r}_{A-2}) - \vec{r}_{A-1}\right], \tag{1d}$$

$$\vec{\xi}_{A-1} = \sqrt{\frac{A-1}{A}}\left[\frac{1}{A-1}(\vec{r}_1 + \vec{r}_2 + \ldots + \vec{r}_{A-1}) - \vec{r}_A\right]. \tag{1e}$$

Here, $\vec{\xi}_0$ is proportional to the c.m. of the A-nucleon system: $\vec{R}=\sqrt{1/A}\vec{\xi}_0$. On the other hand, $\vec{\xi}_\rho$ is proportional to the relative position of the $\rho+1$st nucleon and the c.m. of the ρ nucleons. Let us rewrite the last and the first equation from (1) as

$$\vec{\xi}_{A-1} = \sqrt{\frac{1}{A}}\vec{R}^{A-1}_{\text{c.m.}} - \sqrt{\frac{A-1}{A}}\vec{r}_A, \tag{2a}$$

$$\vec{\xi}_0 = \sqrt{\frac{A-1}{A}}\vec{R}^{A-1}_{\text{c.m.}} + \sqrt{\frac{1}{A}}\vec{r}_A, \tag{2b}$$

where $\vec{R}^{A-1}_{\text{c.m.}}=\sqrt{1/A-1}[\vec{r}_1+\vec{r}_2+\ldots+\vec{r}_{A-1}]$. Following, e.g., Ref. [14], the HO wave functions depending on the coordinates (2) transform as

$$\sum_{M_1 m_1} (L_1 M_1 l_1 m_1 | Qq)\varphi_{N_1 L_1 M_1}(\vec{R}^{A-1}_{\text{c.m.}})\varphi_{n_1 l_1 m_1}(\vec{r}_A) = \sum_{nlmNLM} \langle nlNLQ | N_1 L_1 n_1 l_1 Q\rangle_{1/A-1}(lmLM|Qq) \times \varphi_{nlm}(\vec{\xi}_{A-1})\varphi_{NLM}(\vec{\xi}_0), \tag{3}$$

where $\langle nlNLQ|N_1L_1n_1l_1Q\rangle_{1/(A-1)}$ is the general HO bracket for two particles with the mass ratio $1/(A-1)$.

B. Nuclear density

The nuclear density operator is defined as [15]

$$\rho_{op}(\vec{r}) = \sum_{i=1}^{A} \delta(\vec{r}-\vec{r}_i) = \sum_{i=1}^{A} \frac{\delta(r-r_i)}{rr_i}\sum_{lm} Y_{lm}(\hat{r}_i)Y^*_{lm}(\hat{r}). \tag{4}$$

Its matrix element between an initial and a final state that were obtained in the Cartesian-coordinate single-particle SD basis can be written in the form

$$_{\text{SD}}\langle A\lambda_f J_f M_f|\rho_{op}(\vec{r})|A\lambda_i J_i M_i\rangle_{\text{SD}} = \frac{1}{\hat{J}_f}\sum (J_i M_i K k | J_f M_f) Y^*_{Kk}(\hat{r}) R_{n_1 l_1}(r) R_{n_2 l_2}(r) \times \left\langle l_1 \tfrac{1}{2} j_1 \| Y_K \| l_2 \tfrac{1}{2} j_2\right\rangle \frac{-1}{\hat{K}} \times {}_{\text{SD}}\langle A\lambda_f J_f \| (a^\dagger_{n_1 l_1 j_1}\tilde{a}_{n_2 l_2 j_2})^{(K)} \| A\lambda_i J_i\rangle_{\text{SD}}. \tag{5}$$

Here, $|A\lambda JM\rangle_{\text{SD}}$ is an A-nucleon eigenstate with the angular momentum J and its third component M, $\hat{K}=\sqrt{2K+1}$, and $\tilde{a}_{jm}=(-1)^{j-m}a_{j,-m}$. The λ stands for remaining quantum numbers. The subscript SD refers to the fact that this state was obtained in the Slater determinant basis, i.e., by using a shell-model code, and, consequently, contains the spurious c.m. component. The $R_{nl}(r)$ in Eq. (5) is the radial HO wave function with the oscillator length parameter $b=b_0=\sqrt{\hbar/m\Omega}$, where m is the nucleon mass. Due to our use of the coordinate transformations (1) the oscillator length parameter is the same for all coordinates, i.e., b_0. The term $(-1/\hat{K})_{\text{SD}}\langle A\lambda_f J_f\|(a^\dagger_{n_1 l_1 j_1}\tilde{a}_{n_2 l_2 j_2})^{(K)}\|A\lambda_i J_i\rangle_{\text{SD}}$ represents the standard one-body density matrix elements (OBDME) computed in shell-model codes. The coordinate $\vec{r}$ in (5) is measured from the center of the HO potential well. Clearly, the density given in (5) contains a contribution from the spurious c.m. motion.

The physical density should depend on the coordinate measured from the c.m. of the nucleus, $\vec{r}-\vec{R}$. The corresponding matrix element is obtained by employing the eigenstates depending on the Jacobi coordinates. By modifying the last relation in (4) we get

$$\langle A\lambda_f J_f M_f|\rho_{op}(\vec{r}-\vec{R})|A\lambda_i J_i M_i\rangle = A\left(\frac{A}{A-1}\right)^{3/2}\langle A\lambda_f J_f M_f|\delta(\vec{\xi}-\vec{\xi}_{A-1})|A\lambda_i J_i M_i\rangle, \tag{6}$$

where $\vec{\xi}=-\sqrt{A/(A-1)}(\vec{r}-\vec{R})$, and $\vec{\xi}_{A-1}$ given by Eq. (1e) is reexpressed as $\vec{\xi}_{A-1}=-\sqrt{A/(A-1)}(\vec{r}_A-\vec{R})$. We used the antisymmetry of the eigenstates and the properties of the Dirac delta function. The relationship between the Jacobi coordinate and SD eigenstates is

$$\langle \vec{r}_1 \ldots \vec{r}_A \sigma_1 \ldots \sigma_A \tau_1 \ldots \tau_A | A\lambda JM\rangle_{\text{SD}} = \langle \vec{\xi}_1 \ldots \vec{\xi}_{A-1}\sigma_1 \ldots \sigma_A\tau_1 \ldots \tau_A | A\lambda JM\rangle \varphi_{000}(\vec{\xi}_0), \tag{7}$$

with σ and τ the spin and isospin coordinates, respectively.

Similarly as in (5), the physical density (6) can be related to "one-body" density matrix elements derived from the Jacobi-coordinate eigenstates (discussed, e.g., in Appendix B of Ref. [13]). In particular, we obtain

$$\langle A\lambda_f J_f M_f|\rho_{op}(\vec{r}-\vec{R})|A\lambda_i J_i M_i\rangle$$
$$= A\left(\frac{A}{A-1}\right)^{3/2}\hat{J}_i\sum(J_iM_iKk|J_fM_f)Y^*_{Kk}(\widehat{\vec{r}-\vec{R}})$$
$$\times R_{nl}\left(\sqrt{\frac{A}{A-1}}|\vec{r}-\vec{R}|\right)R_{n'l'}\left(\sqrt{\frac{A}{A-1}}|\vec{r}-\vec{R}|\right)$$
$$\times\left\langle l\tfrac{1}{2}j\|Y_K\|l'\tfrac{1}{2}j'\right\rangle(-1)^{J_{\mathrm{A}-1}+J_f+j'}\begin{Bmatrix}J_{\mathrm{A}-1} & j' & J_i\\ K & J_f & j\end{Bmatrix}$$
$$\times\langle A\lambda_f J_f|(N_{\mathrm{A}-1}i_{\mathrm{A}-1}J_{\mathrm{A}-1};nlj)\,J_f\rangle$$
$$\times\langle(N_{\mathrm{A}-1}i_{\mathrm{A}-1}J_{\mathrm{A}-1};n'l'j')J_i|A\lambda_i J_i\rangle. \quad (8)$$

Here the eigenstates are expanded in a basis with a lower degree of antisymmetry using the coefficients of fractional parentage [13],

$$\langle(N_{\mathrm{A}-1}i_{\mathrm{A}-1}J_{\mathrm{A}-1};nlj)J|A\lambda J\rangle=\sum\langle N_{\mathrm{A}-1}i_{\mathrm{A}-1}J_{\mathrm{A}-1};nlj\|NiJ\rangle$$
$$\times\langle NiJ|A\lambda J\rangle, \quad (9)$$

with $N=N_{\mathrm{A}-1}+2n+l$ the total number of HO excitations for the A nucleons and $i,i_{\mathrm{A}-1}$ the additional quantum numbers that characterize the A- and $(A-1)$-nucleon antisymmetrized basis states, respectively.

C. Physical density in terms of the SD OBDME

It turns out that obtaining the eigenstates (9) becomes increasingly difficult with the number of nucleons A, mostly due to the complicated antisymmetrization. As stated in Sec. I for $A>4$ it is by far more efficient to use the SD basis. Consequently, it is desirable to relate the matrix element (6) to the SD OBDME $(-1/\hat{K})_{\mathrm{SD}}\langle A\lambda_f J_f\|(a^\dagger_{n_1l_1j_1}\tilde{a}_{n_2l_2j_2})^{(K)}\|A\lambda_i J_i\rangle_{\mathrm{SD}}$.

Let us note that an intermediate result that eventually leads to the right-hand side of Eq. (8) reads

$$\langle A\lambda_f J_f M_f|\rho_{op}(\vec{r}-\vec{R})|A\lambda_i J_i M_i\rangle$$
$$= A\left(\frac{A}{A-1}\right)^{3/2}\sum R_{nl}(\xi)R_{n'l'}(\xi)\frac{\hat{l}\hat{l}'}{\sqrt{4\pi}\hat{K}}(l0l'0|K0)$$
$$\times Y^*_{Kk}(\hat{\xi})(lml'm'|Kk)\int d\vec{\xi}_1\ldots d\vec{\xi}_{A-2}d\vec{\xi}_{A-1}d\vec{\xi}'_{A-1}$$
$$\times\langle A\lambda_f J_f M_f|\vec{\xi}_1\ldots\vec{\xi}_{A-1}\rangle\varphi_{nlm}(\vec{\xi}_{A-1})\varphi_{n'l'm'}(\vec{\xi}'_{A-1})$$
$$\times\langle\vec{\xi}_1\ldots\vec{\xi}_{A-2}\vec{\xi}'_{A-1}|A\lambda_i J_i M_i\rangle, \quad (10)$$

where for simplicity we suppress from now on spin and isospin coordinates. In deriving Eq. (10) we used the Dirac delta function properties and the relation $\delta(\vec{\xi}-\vec{\xi}_{A-1})=\Sigma_{nlm}\varphi_{nlm}(\vec{\xi}_{A-1})\varphi^*_{nlm}(\vec{\xi})$.

We now investigate an analogous integral to that appearing on the right-hand side of Eq. (10) for the Cartesian-coordinate wave functions and, as the first result, we relate it to the OBDME,

$$\sum_{\sigma_i\tau_i m_1m_2}(l_1m_1l_2m_2|Kk)\int d\vec{r}_1\ldots d\vec{r}_{A-1}d\vec{r}_A d\vec{r}'_A$$
$$\times_{\mathrm{SD}}\langle A\lambda_f J_f M_f|\vec{r}_1\ldots\vec{r}_A\rangle\varphi_{n_1l_1m_1}(\vec{r}_A)\varphi_{n_2l_2m_2}(\vec{r}'_A)$$
$$\times\langle\vec{r}_1\ldots\vec{r}_{A-1}\vec{r}'_A|A\lambda_i J_i M_i\rangle_{\mathrm{SD}}$$
$$=\frac{1}{A}\sum\nolimits_{j_1j_2\,\mathrm{SD}}\langle A\lambda_f J_f M_f|(a^\dagger_{n_1l_1j_1}\tilde{a}_{n_2l_2j_2})^{(K)}_k|A\lambda_i J_i M_i\rangle_{\mathrm{SD}}$$
$$\times(-1)^{l_1+l_2+K+j_2-1/2}\hat{j}_1\hat{j}_2\begin{Bmatrix}j_1 & j_2 & K\\ l_2 & l_1 & \frac{1}{2}\end{Bmatrix}. \quad (11)$$

Next, we rewrite the left-hand side of Eq. (11) and perform a change of variables to the Jacobi coordinates,

$$\sum_{\sigma_i\tau_i m_1m_2}(l_1m_1l_2m_2|Kk)\int d\vec{r}_1\ldots d\vec{r}_{A-1}d\vec{r}_A d\vec{r}'_1\ldots d\vec{r}'_{A-1}d\vec{r}'_{A\mathrm{SD}}\langle A\lambda_f J_f M_f|\vec{r}_1\ldots\vec{r}_A\rangle\varphi_{n_1l_1m_1}(\vec{r}_A)\varphi_{n_2l_2m_2}(\vec{r}'_A)$$
$$\times\delta(\vec{r}_1-\vec{r}'_1)\ldots\delta(\vec{r}_{A-1}-\vec{r}'_{A-1})\langle\vec{r}'_1\ldots\vec{r}'_{A-1}\vec{r}'_A|A\lambda_i J_i M_i\rangle_{\mathrm{SD}}$$
$$=\sum_{\sigma_i\tau_i m_1m_2}(l_1m_1l_2m_2|Kk)\int d\vec{\xi}_1\ldots d\vec{\xi}_{A-2}d\vec{R}^{A-1}_{\mathrm{c.m.}}d\vec{r}_A d\vec{\xi}'_1\ldots d\vec{\xi}'_{A-2}d\vec{R}'^{A-1}_{\mathrm{c.m.}}d\vec{r}'_A\langle A\lambda_f J_f M_f|\vec{\xi}_1\ldots\vec{\xi}_{A-1}\rangle\varphi^*_{000}(\vec{\xi}_0)$$
$$\times\varphi_{n_1l_1m_1}(\vec{r}_A)\varphi_{n_2l_2m_2}(\vec{r}'_A)\delta(\vec{\xi}_1-\vec{\xi}'_1)\ldots\delta(\vec{\xi}_{A-2}-\vec{\xi}'_{A-2})\delta(\vec{R}^{A-1}_{\mathrm{c.m.}}-\vec{R}'^{A-1}_{\mathrm{c.m.}})\varphi_{000}(\vec{\xi}'_0)\langle\vec{\xi}'_1\ldots\vec{\xi}'_{A-1}|A\lambda_i J_i M_i\rangle$$
$$=\sum_{\sigma_i\tau_i m_1m_2}(l_1m_1l_2m_2|Kk)\int d\vec{\xi}_1\ldots d\vec{\xi}_{A-2}d\vec{R}^{A-1}_{\mathrm{c.m.}}d\vec{r}_A d\vec{R}'^{A-1}_{\mathrm{c.m.}}d\vec{r}'_A\langle A\lambda_f J_f M_f|\vec{\xi}_1\ldots\vec{\xi}_{A-1}\rangle\varphi^*_{000}(\vec{\xi}_0)$$
$$\times\varphi_{n_1l_1m_1}(\vec{r}_A)\varphi_{N_1L_1M_1}(\vec{R}^{A-1}_{\mathrm{c.m.}})(-1)^{m_2}\varphi^*_{n_2l_2-m_2}(\vec{r}'_A)\varphi^*_{N_1L_1M_1}(\vec{R}'^{A-1}_{\mathrm{c.m.}})\varphi_{000}(\vec{\xi}'_0)\langle\vec{\xi}_1\ldots\vec{\xi}_{A-2}\vec{\xi}'_{A-1}|A\lambda_i J_i M_i\rangle$$
$$=\sum_{\sigma_i\tau_i nlmn'l'm'N_1L_1}(-1)^{l+l'+K+L_1}\begin{Bmatrix}l_1 & L_1 & l\\ l' & K & l_2\end{Bmatrix}\hat{l}\hat{l}'\langle nl00l|N_1L_1n_1l_1l\rangle_{1/(A-1)}\langle n'l'00l'|N_1L_1n_2l_2l'\rangle_{1/(A-1)}(lml'm'|Kk)$$
$$\times\int d\vec{\xi}_1\ldots d\vec{\xi}_{A-2}d\vec{\xi}_{A-1}d\vec{\xi}'_{A-1}\langle A\lambda_f J_f M_f|\vec{\xi}_1\ldots\vec{\xi}_{A-1}\rangle\varphi_{nlm}(\vec{\xi}_{A-1})\varphi_{n'l'm'}(\vec{\xi}'_{A-1})\langle\vec{\xi}_1\ldots\vec{\xi}_{A-2}\vec{\xi}'_{A-1}|A\lambda_i J_i M_i\rangle. \quad (12)$$

In the above derivation, we used the relations (1)–(3) and (7) together with

$$\delta(\vec{R}^{A-1}_{\rm c.m.} - \vec{R}'^{A-1}_{\rm c.m.}) = \sum_{N_1L_1M_1} \varphi_{N_1L_1M_1}(\vec{R}^{A-1}_{\rm c.m.})\varphi^*_{N_1L_1M_1}(\vec{R}'^{A-1}_{\rm c.m.}).$$

The last term in Eq. (12) contains the integral appearing on the right-hand side of Eq. (10). We can now relate this integral to the OBDME, i.e., the right-hand side of Eq. (11). In order to do that, we define a matrix

$$\begin{aligned}(M^K)_{n_1l_1n_2l_2,nln'l'} &= \sum_{N_1L_1} (-1)^{l+l'+K+L_1} \\ &\times \begin{Bmatrix} l_1 & L_1 & l \\ l' & K & l_2 \end{Bmatrix} \hat{l}\hat{l}' \langle nl00l|N_1L_1n_1l_1l\rangle_{1/(A-1)} \\ &\times \langle n'l'00l'|N_1L_1n_2l_2l'\rangle_{1/(A-1)}. \end{aligned} \tag{13}$$

As we are interested only in the case when $(-)^{l+l'+K} = (-1)^{l_1+l_2+K} = 1$, the above definition assumes this restriction.

Then, by inverting the matrix M^K we obtain

$$\begin{aligned}&\sum_{\sigma_i\tau_i mm'} (lml'm'|Kk) \int d\vec{\xi}_1 \ldots d\vec{\xi}_{A-2} d\vec{\xi}_{A-1} d\vec{\xi}'_{A-1} \\ &\times \langle A\lambda_f J_j M_f|\vec{\xi}_1 \ldots \vec{\xi}_{A-1}\rangle \varphi_{nlm}(\vec{\xi}_{A-1}) \varphi_{n'l'm'}(\vec{\xi}'_{A-1}) \\ &\times \langle \vec{\xi}_1 \ldots \vec{\xi}_{A-2}\vec{\xi}'_{A-1}|A\lambda_i J_i M_i\rangle \\ &= \frac{1}{A}\sum_{n_1l_1j_1n_2l_2j_2} (M^K)^{-1}_{nln'l',n_1l_1n_2l_2} \\ &\times {}_{\rm SD}\langle A\lambda_f J_f M_f|(a^\dagger_{n_1l_1j_1}\tilde{a}_{n_2l_2j_2})^{(K)}_k|A\lambda_i J_i M_i\rangle_{\rm SD} \\ &\times (-1)^{l_1+l_2+K+j_2-1/2}\hat{j}_1\hat{j}_2 \begin{Bmatrix} j_1 & j_2 & K \\ l_2 & l_1 & \frac{1}{2} \end{Bmatrix}. \end{aligned} \tag{14}$$

Eventually, with the help of

$$\begin{aligned}\langle l_1\tfrac{1}{2}j_1\|Y_K\|l_2\tfrac{1}{2}j_2\rangle &= \frac{1}{\sqrt{4\pi}}\hat{j}_1\hat{j}_2\hat{l}_1\hat{l}_2(-1)^{j_2+1/2}(l_10l_20|K0) \\ &\times \begin{Bmatrix} j_1 & j_2 & K \\ l_2 & l_1 & \frac{1}{2} \end{Bmatrix} \end{aligned} \tag{15}$$

for the spherical harmonics matrix element, we arrive at the main result of this paper,

$$\begin{aligned}&\langle A\lambda_f J_f M_f|\rho_{op}(\vec{r}-\vec{R})|A\lambda_i J_i M_i\rangle \\ &= \left(\frac{A}{A-1}\right)^{3/2}\frac{1}{\hat{j}_f}\sum (J_iM_iKk|J_fM_f) Y^*_{Kk}(\widehat{\vec{r}-\vec{R}}) \\ &\times R_{nl}\left(\sqrt{\frac{A}{A-1}}|\vec{r}-\vec{R}|\right) R_{n'l'}\left(\sqrt{\frac{A}{A-1}}|\vec{r}-\vec{R}|\right) \\ &\times (-1)^K \frac{\hat{l}\hat{l}'(l0l'0|K0)}{\hat{l}_1\hat{l}_2(l_10l_20|K0)}(M^K)^{-1}_{nln'l',n_1l_1n_2l_2} \\ &\times \langle l_1\tfrac{1}{2}j_1\|Y_K\|l_2\tfrac{1}{2}j_2\rangle \frac{-1}{\hat{K}} \\ &\times {}_{\rm SD}\langle A\lambda_f J_f\|(a^\dagger_{n_1l_1j_1}\tilde{a}_{n_2l_2j_2})^{(K)}\|A\lambda_i J_i\rangle_{\rm SD}, \end{aligned} \tag{16}$$

with the sum restricted to both $l+l'+K$ and l_1+l_2+K even. Equation (16) is the desired relation between the physical translationally invariant density and the OBDME obtained in the SD basis.

D. Properties

All the derivations presented in the Secs. II A–II C were performed for a nucleon density. It should be noted that Eq. (16) is trivially generalized to obtain the proton and neutron densities separately. The relation (14) involves spatial transformations and remains valid even if we add spin or isospin operators. Similarly, Eq. (16) is readily generalizable for a case of a nonlocal density that is needed as an input for some semimicroscopic optical potential folding approaches, see, e.g., Ref. [16].

The physical density (8) and (16), as well as the shell-model density (5), are normalized as

$$\begin{aligned}&\int d\vec{x}\langle A\lambda JM|\rho^{\rm phys}_{op}(\vec{x})|A\lambda JM\rangle \\ &= \int d\vec{x}_{\rm SD}\langle A\lambda JM|\rho^{\rm SM}_{op}(\vec{x})|A\lambda JM\rangle_{\rm SD} = A, \end{aligned} \tag{17}$$

where the superscripts "phys" and "SM" refer to Eqs. (8), (16), and (5), respectively.

We note that the point-nucleon matter radius is obtained only by using the physical density,

$$\begin{aligned}r^2_m &= \langle A\lambda JM|\frac{1}{A}\sum_{i=1}^A (\vec{r}_i - \vec{R})^2|A\lambda JM\rangle \\ &= \frac{1}{A}\int d\vec{x}x^2\langle A\lambda JM|\rho^{\rm phys}_{op}(\vec{x})|A\lambda JM\rangle. \end{aligned} \tag{18}$$

The analogous integral for the shell-model density gives a value different from the point-nucleon matter radius, as it contains a contribution from the spurious c.m.

Equation (16) above can be compared to Eq. (7) of Ref. [9] and, similarly, Eq. (5) to Eq. (6) of Ref. [9]. In Ref. [9], the transformation that removes the c.m. components was made by inserting a complete set of nonspurious shell-model eigenstates between the $a^\dagger$ and a operators, which introduces the familiar $(A/(A-1))^{(2n+l)/2}$ factors that relate matrix elements in coordinates referred to the arbitrary origin and the $(A-1)$ core. The present result is more general, as a direct relation to the OBDME was found and, consequently, no sum of intermediate states is needed.

III. APPLICATION TO ^{6}He

We tested the physical translationally invariant density formulas (8) and (16) by performing identical calculations for ^{3}H, ^{4}He, and ^{5}He in the Jacobi-coordinate HO basis and the SD HO basis, respectively. The Jacobi-coordinate HO basis calculations were performed using the code MANYEFF [13] that constructs the A-nucleon antisymmetrized Jacobi-coordinate HO basis, calculates the effective interaction from a nucleon-nucleon (NN) potential, and, eventually, finds the A-nucleon eigenvalues and wave functions. These wave

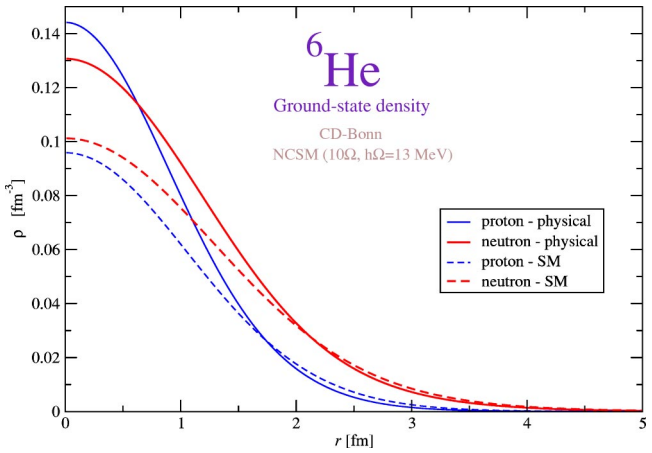

FIG. 1. (Color online) ^{6}He proton and neutron monopole-ground state densities obtained in the $10\hbar\Omega$ basis space and the HO frequency of $\hbar\Omega=13$ MeV. The NCSM two-body effective interaction was derived from the CD-Bonn *NN* potential. The full lines correspond to the physical densities calculated according to Eq. (16), while the dashed lines correspond to the shell-model densities [Eq. (5)] that contain the spurious center-of-mass contribution.

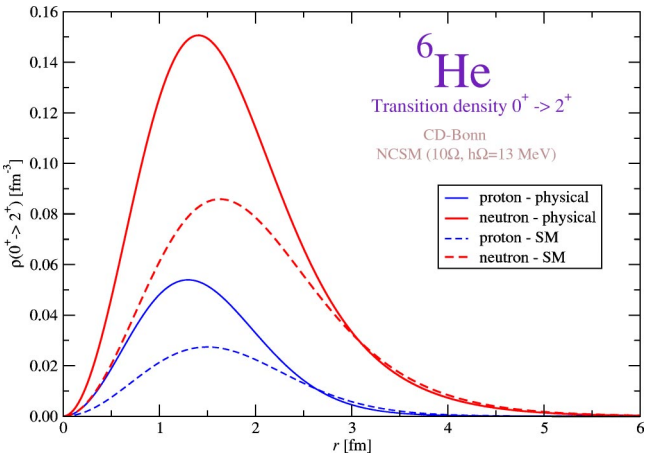

FIG. 2. (Color online) ^{6}He proton and neutron quadrupole transition densities from the ground state to the first excited 2^+ state obtained in the $10\hbar\Omega$ basis space and the HO frequency of $\hbar\Omega=13$ MeV. The NCSM two-body effective interaction was derived from the CD-Bonn *NN* potential. The full lines correspond to the physical densities calculated according to Eq. (16), while the dashed lines correspond to the shell-model densities [Eq. (5)] that contain the spurious center-of-mass contribution.

functions were then employed to calculate physical density according to Eq. (8). The same effective interaction, transformed to the single-particle basis, was used in the SD HO basis calculation using the many-fermion dynamics (MFD) [17] shell-model code. A specialized code was then used to calculate the OBDME from the MFD eigenfunctions, and eventually, the physical density was calculated by applying Eq. (16). We obtained identical results in the two independent calculations.

As an illustration of the significance of the spurious c.m. removal, we calculated the ^{6}He physical (16) and the shell-model (5) densities using wave functions obtained in Ref. [18]. In Fig. 1, the proton and neutron monopole ground-state densities are shown. A $10\hbar\Omega$ basis space and the HO frequency of $\hbar\Omega=13$ MeV was used. The two-body-effective interaction was derived from the CD-Bonn *NN* potential. The full lines correspond to the physical densities calculated according to Eq. (16), while the dashed lines correspond to the shell-model densities (5) that contain the spurious c.m. contribution. Obviously, the same OBDME were employed in both calculations. The normalization of the densities in Fig. 1 is $4\pi\int drr^2\rho_{K=0,p(n)}(r)=Z(N)$, where p, n refers to the proton and neutron, respectively, and $\rho_{K=0}(r)=1/4\pi\int d\hat{r}\langle A\lambda JM|\rho_{op}(\vec{r})|A\lambda JM\rangle$. One can clearly see substantial differences between the two sets of densities, in particular, at short distances. By performing the integral (18) for the physical density we indeed recover to point-proton and point-neutron rms radii 1.763 and 2.361 fm, respectively [18]. Performing the same integral using the shell-model densities gives incorrect, larger radii 1.976 and 2.524 fm, respectively. The difference between the squares of the two sets of radii is equal to the mean value of the c.m. $\vec{R}^2$, i.e., $_{\rm SD}\langle A\lambda JM|\vec{R}^2|A\lambda JM\rangle_{\rm SD}=(1/A)\langle 000|\vec{\xi}_0^2|000\rangle=0.798$ fm^2.

In Figs. 2 and 3 we present transition densities from the ^{6}He ground state to the first excited 2^+ state and the lowest 1^- ("soft-dipole mode") state, respectively. The $10\hbar\Omega$ basis space was employed for the $0^+\rightarrow 2^+$ case, while the $8\hbar\Omega$ (for the ground state) and the $9\hbar\Omega$ (for the 1^- state) basis were utilized for the $0^+\rightarrow 1^-$ transition. In both cases we can see substantial differences between the physical (16) and shell-model (5) densities. By integrating the proton densities, one obtains the reduced *EK* matrix element,

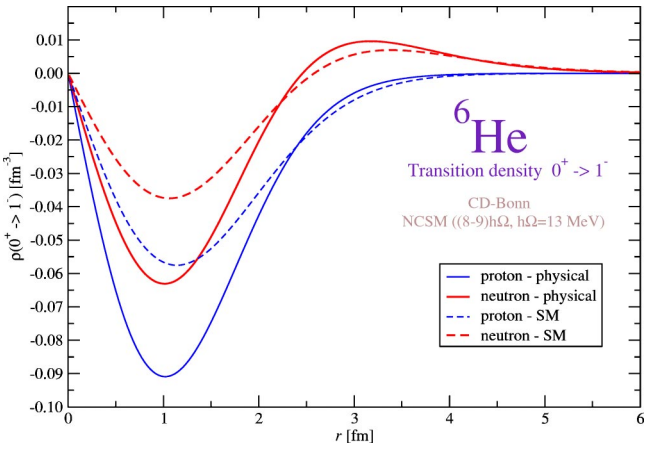

FIG. 3. (Color online) ^{6}He proton and neutron dipole transition densities from the ground state to the lowest 1^- state obtained in the $(8-9)\hbar\Omega$ basis space and the HO frequency of $\hbar\Omega=13$ MeV. The NCSM two-body effective interaction was derived from the CD-Bonn *NN* potential. The full lines correspond to the physical densities calculated according to Eq. (16), while the dashed lines correspond to the shell-model densities [Eq. (5)] that contain the spurious center-of-mass contribution.

$$\int d\vec{x} x^K Y_{K,M_f-M_i}(\hat{x}) \langle A\lambda_f J_f M_f | \rho^{\rm phys}_{op,p}(\vec{x}) | A\lambda_i J_i M_i \rangle$$

$$= \frac{1}{\hat{J}_f} (J_i M_i K M_f - M_i | J_f M_f) M(EK; J_i \to J_f), \qquad (19)$$

with $B(EK; J_i \to J_f) = [1/(2J_i+1)] |M(EK; J_i \to J_f)|^2$. Here, the bare nucleon charges are assumed ($e_p=1, e_n=0$). The result of the integral (19) is unchanged for the shell-model densities, i.e., when the matrix element (16) is replaced by the matrix element (5) in Eq. (19). In the present particular cases we obtain $B(E2; 0^+ \to 2^+) = 1.056\ e^2\ \text{fm}^4$ and $B(E1; 0^+ \to 1^-) = 0.388\ e^2\ \text{fm}^2$, in agreement with the results found in Ref. [18]. The normalization of the densities in Figs. 2 and 3 is $\int dr r^{2+K} \rho_{K,p}(r) = M(EK)$ for the proton case and similarly for the neutron case. Here,

$$\rho_K(r) = \hat{J}_f \sum_{M_i k} (J_i M_i K k | J_f M_f) \times \int d\hat{r} Y_K(\hat{r})\ \langle A\lambda_f J_f M_f | \rho_{op}(\vec{r}) | A\lambda_i J_i M_i \rangle .$$

It has been argued that the spin-orbit component of the nucleon-nucleus optical potential is proportional to the derivative of the monopole density [19]. The following form of the potential that takes into account the isovector component is typically considered

$$V_{\rm so}(r) = -(\pi/3) V_s \frac{1}{r} \frac{d}{dr} [2\rho_{K=0,p}(r) + \rho_{K=0,n}(r)] \vec{l} \cdot \vec{\sigma}, \qquad (20)$$

for the proton-nucleus potential, with the p and n indexes exchanged for the neutron-nucleus potential. In Eq. (20), V_s (typically $V_s < 0$) is a constant. We calculated the proton-^{6}He spin-orbit optical potential according to Eq. (20) using the ^{6}He ground-state monopole densities shown in Fig. 1. The resulting shape of the spin-orbit potential, $\frac{1}{3}(1/r)(d/dr)[2\rho_{K=0,p}(r) + \rho_{K=0,n}(r)]$, is presented in Fig. 4. In particular, we compare the result obtained using the physical density (16) with that obtained using the shell-model density (5) that includes the spurious c.m. contribution. Clearly, the differences of the densities as seen in Fig. 1 are even more magnified in the shape of spin-orbit potential. Such differences must have an impact on observables, like analyzing powers calculated using these spin-orbit potentials. In order to obtain meaningful results, one must employ the physical density to construct the spin-orbit component of the optical potential.

IV. CONCLUSIONS

In this paper, the translationally invariant nuclear density was derived from the shell-model one-body densities by removing their spurious $0\hbar\Omega$ c.m. motion component. The main result of this paper, presented in Eq. (16) relates the translationally invariant density to the OBDME calculated in the shell-model codes by employing the second-quantization techniques. This is important for the NCSM approach, as calculations for $A > 4$ are much more efficiently performed in the Cartesian-coordinate SD basis, which has the down side of contaminating the wave functions by the spurious c.m. components. As the NCSM effective interaction is translationally invariant, and for the basis space a complete $N_{\rm max}\hbar\Omega$ space is used, these components can always be exactly removed. In this paper, this was achieved for the density, a case less trivial compared to other operators. This paves the way to utilize the *ab initio* no-core shell-model nuclear structure in folding approaches to optical potentials.

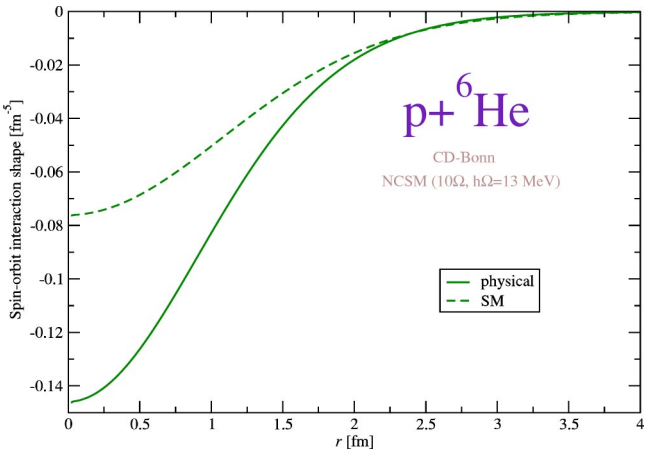

FIG. 4. (Color online) The shape of the proton-^{6}He spin-orbit optical potential, $\frac{1}{3}(1/r)(d/dr)[2\rho_{K=0,p}(r) + \rho_{K=0,n}(r)]$, obtained using the ground-state ^{6}He densities from the $10\hbar\Omega$, $\hbar\Omega = 13$ MeV NCSM calculation. The two-body effective interaction was derived from the CD-Bonn *NN* potential. The full lines correspond to the physical densities calculated according to Eq. (16), while the dashed lines correspond to the shell-model densities [Eq. (5)] that contain the spurious center-of-mass contribution.

We performed tests of the present formalism by performing independent calculations using the Jacobi-coordinate HO basis and the Cartesian-coordinate HO SD basis for ^{3}H, ^{4}He and ^{5}He. Identical results for the densities were obtained.

As an illustration, the ^{6}He diagonal and transitional densities were calculated from the NCSM wave functions obtained using the CD-Bonn nucleon-nucleon potential in the $10\hbar\Omega$ basis space. These densities were compared to those obtained without the spurious c.m. component removal. Substantial differences were found for both the diagonal monopole and the transitional multipole densities. Only using the physical density one can recover the point-nucleon matter radius. On the other hand, the *EK* reduced matrix elements can be obtained using both the physical and the uncorrected density. A particularly significant impact of the exact removal of the spurious c.m. motion was found for the spin-orbit part of the optical potential proportional to the derivative of the nuclear density.

The physical density can now be used in folding approaches to nucleon-nucleus optical potentials, such as those described, e.g., in Refs. [11,16], and subsequently applied in the coupled-channel calculations. Work in this direction is under way.

ACKNOWLEDGMENTS

The author thanks D. J. Millener for useful comments. This work was performed under the auspices of the U.S. Department of Energy by the University of California, Lawrence Livermore National Laboratory under Contract No. W-7405-Eng-48. Partial support from the LDRD Contract No. 04-ERD-058 is acknowledged.

[1] B. S. Pudliner, V. R. Pandharipande, J. Carlson, S. C. Pieper, and R. B. Wiringa, Phys. Rev. C **56**, 1720 (1997); R. B. Wiringa, S. C. Pieper, J. Carlson, and V. R. Pandharipande, *ibid.* **62**, 014001 (2000); S. C. Pieper, K. Varga, and R. B. Wiringa, Annu. Rev. Nucl. Part. Sci. **51**, 53 (2001); Phys. Rev. C **66**, 044310 (2002).

[2] P. Navrátil, J. P. Vary, and B. R. Barrett, Phys. Rev. Lett. **84**, 5728 (2000); Phys. Rev. C **62**, 054311 (2000).

[3] E. Caurier, G. Martinez-Pinedo, F. Nowacki, A. Poves, J. Retamosa, and A. P. Zuker, Phys. Rev. C **59**, 2033 (1999); E. Caurier and F. Nowacki, Acta Phys. Pol. B **30**, 705 (1999).

[4] L. J. Tassie and F. C. Barker, Phys. Rev. **111**, 940 (1958).

[5] A. E. L. Dieperink and T. de Forest, Jr., Phys. Rev. C **10**, 543 (1974).

[6] Taber de Forest, Jr., Phys. Rev. C **22**, 2222 (1980).

[7] R. J. Philpott, Nucl. Phys. **A289**, 109 (1977).

[8] Dean Halderson and R. J. Philpott, Nucl. Phys. **A321**, 295 (1979).

[9] D. J. Millener, J. W. Olness, E. K. Warburton, and S. S. Hanna, Phys. Rev. C **28**, 497 (1983).

[10] F. P. Brady, T. D. Ford, G. A. Needham, J. L. Romero, D. S. Sorenson, C. M. Castaneda, J. L. Drummond, E. L. Hjort, B. McEachern, N. S. P. King, and D. J. Millener, Phys. Rev. C **43**, 2284 (1991).

[11] J.-P. Jeukenne, A. Lejeune, and C. Mahaux, Phys. Rev. C **16**, 80 (1977).

[12] I. J. Thompson, Comput. Phys. Rep. **7**, 167 (1988).

[13] P. Navrátil, G. P. Kamuntavičius, and B. R. Barrett, Phys. Rev. C **61**, 044001 (2000).

[14] L. Trlifaj, Phys. Rev. C **5**, 1534 (1972).

[15] G. R. Satchler, *Direct Nuclear Reactions* (Oxford University Press, Oxford, 1983).

[16] K. Amos, P. J. Dortmans, H. V. von Geramb, S. Karataglidis, and J. Raynal, Adv. Nucl. Phys. **25**, 275 (2000).

[17] J. P. Vary, The Many-Fermion-Dynamics Shell-Model Code, Iowa State University, 1992 (unpublished); J. P. Vary and D. C. Zheng, The Many-Fermion-Dynamics Shell-Model Code, Iowa State University, 1994.

[18] P. Navrátil, J. P. Vary, W. E. Ormand, and B. R. Barrett, Phys. Rev. Lett. **87**, 172502 (2001).

[19] R. R. Scheerbaum, Nucl. Phys. **A257**, 77 (1976); F. A. Brieva and J. R. Rook, *ibid.* **A297**, 206 (1978); Ch. Lagrange, D. G. Madland, and M. Girod, Phys. Rev. C **33**, 1616 (1986); E. Bauge, J. P. Delaroche, and M. Girod, *ibid.* **58**, 1118 (1998).